Technological University Dublin
ARROW@TU Dublin

Conference papers | School of Electrical and Electronic Engineering

2009-09-04

The Integrated Control of the Rotor Side and Grid Side Converters in a DFIG to Reduce Both Power and Torque Pulsations During Network Voltage Unbalance Conditions.

Joseph Kearney
Technological University Dublin, joseph.kearney@tudublin.ie

Michael Conlon
Technological University Dublin, michael.conlon@tudublin.ie

Eugene Coyle
Technological University Dublin, Eugene.Coyle@tudublin.ie

Follow this and additional works at: https://arrow.tudublin.ie/engscheleart

Part of the Electrical and Electronics Commons, and the Power and Energy Commons

Recommended Citation

Kearney, Joseph; Conlon, Michael; and Coyle, Eugene, "The Integrated Control of the Rotor Side and Grid Side Converters in a DFIG to Reduce Both Power and Torque Pulsations During Network Voltage Unbalance Conditions." (2009). *Conference papers*. 221.
https://arrow.tudublin.ie/engscheleart/221

This Conference Paper is brought to you for free and open access by the School of Electrical and Electronic Engineering at ARROW@TU Dublin. It has been accepted for inclusion in Conference papers by an authorized administrator of ARROW@TU Dublin. For more information, please contact arrow.admin@tudublin.ie, aisling.coyne@tudublin.ie, vera.kilshaw@tudublin.ie.

The Integrated Control of the Rotor Side and Grid Side Converters in a DFIG to Reduce Both Power and Torque Pulsations During Network Voltage Unbalance Conditions.

Joseph Kearney
Dublin Institute of Technology, Ireland
Joseph.kearney@dit.ie

Michael F Conlon
Dublin Institute of Technology, Ireland
Michael.Conlon@dit.ie

Eugene Coyle
Dublin Institute of Technology, Ireland
Eugene.Coyle@dit.ie

Abstract- **The paper describes a method to control the rotor-side and grid side converters in a DFIG when subjected to the effects of network voltage unbalance conditions. In particular the control scheme of the grid side converter is adapted to assist in the control of the total power oscillations when the rotor side converter is controlling the DFIG torque pulsations. A DFIG model is implemented in Matlab/Simulink and simulations show the reduction in power and torque oscillations and a reduction in the high unbalanced currents generated as a result of the applied voltage unbalance.**

***Index Terms*—DFIG, Voltage Unbalance, Wind Energy**

I. Introduction

The most productive sites for the development of wind turbines and wind farms are in remote rural areas where distribution networks can be weak and voltage unbalance can be a common feature. Network voltage unbalance is a power quality problem that can affect wind turbines. Voltage unbalance can give rise to excessive unbalanced stator and rotor currents in DFIG's and overloading of the rotor converter causing generators to trip out [9]. Mechanical stress can also occur due to torque pulsations.

This paper considers measures, which are available to alleviate the effects of voltage unbalance. The process involves modifying the standard DFIG control structures of both the rotor side and grid converter and introducing parallel negative sequence control routines to compensate for negative sequence voltage. This is required in both the rotor-side converter and the grid-side converter.

Normally when controlling the rotor-side converter for the reduction of stator power and torque pulsations due to grid voltage unbalance it was not possible to reduce both the power and torque pulsations simultaneously, due to the limitations of the control variables. The method investigated in this paper integrates the control variables of both the rotor-side and grid-side converters in a coordinated fashion and shows it is possible to reduce both the DFIG power and torque pulsations. Improvements in the control structures of the rotor side and grid side converters are investigated, and simulations performed in Matlab/Simulink to outline the improvements in the performance of the DFIG.

II. Simulation Study

The DFIG wind turbine in this study is modelled in Matlab/Simulink [2] to analyse the behaviour of the DFIG to grid voltage unbalance.

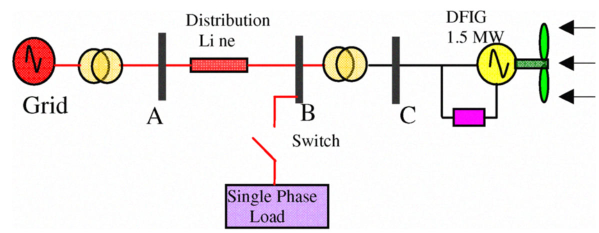

Fig. 1. DFIG and Network Model

The system under investigation is shown in Fig. 1 and further details can be obtained in [9]. As shown in Fig. 1, a single-phase load is supplied at bus B. In the model when the switch is closed this single-phase load introduces a voltage unbalance of 5% at Bus B. The voltage unbalance is expressed as the ratio of the negative sequence voltage to the positive sequence voltage [3].

III. Method of Controlling DFIG During Voltage Unbalance Conditions

The DFIG consists of an induction generator and a back-to-back PWM converter consisting of a rotor side and grid converter. Network voltage unbalance not only affects the induction generator but also the PWM converter in the rotor [9]. The rotor side converter normally controls the real power and reactive power supplied to the network, whereas the grid side converter controls the dc link bus voltage and can also influence the power factor [1].

To reduce the power and torque pulsations as a result of network voltage unbalance it is necessary to modify the control structure of the rotor side converter. The traditional control structure of a DFIG can be modified to incorporate routines for positive and negative sequence control [4, 7, 9]. The idea is to control the positive and negative sequence components independently.

In an unbalanced network the stator apparent power can be expressed in terms of positive and negative sequence components [4, 5, 6]. Due to these components it is necessary to analyse the DFIG per-phase equivalent circuit in the positive and negative sequence dq reference frames.

The positive and negative reference frames can be described by Fig. 2, where both the rotor side converter and

978-0-947649-44-9/09/$26.00 ©2009 IEEE

grid side converter are controlled in the SVO, stator voltage reference frame. Observing Fig. 2 the transformation between $\alpha\beta$, dq^+ and dq^- reference frames is given as [4, 6]:

$$V_{dq}^{+} = V_{\alpha\beta} e^{-j\omega_e t}, \qquad V_{dq}^{-} = V_{\alpha\beta} e^{j\omega_e t} \tag{1}$$

$$V_{dq}^{+} = V_{dq}^{-} e^{-2j\omega_e t}, \qquad V_{dq}^{-} = V_{dq}^{+} e^{2j\omega_e t} \tag{2}$$

where superscripts (+) and (–) represent the positive and negative sequence reference frames, respectively.

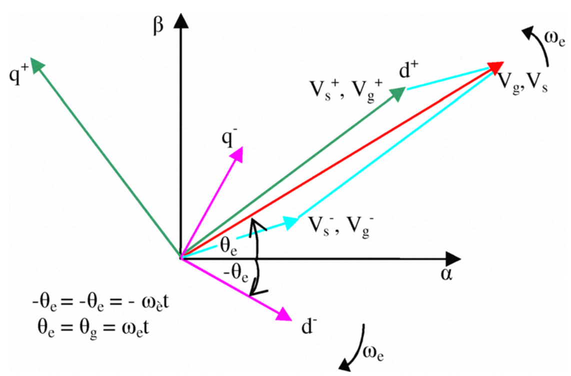

Fig. 2. Positive & Negative Sequence dq Reference Frames

Observing Fig. 2, (1) and (2) the stator voltage vectors can be expressed using their respective positive and negative sequence components as:

$$V_{dqs}^{+} = V_{dqs+}^{+} + V_{dqs-}^{+} = V_{dqs+}^{+} + V_{dqs-}^{-}.e^{-2j\omega_e t} \tag{3}$$

$$V_{dqs}^{-} = V_{dqs-}^{-} + V_{dqs+}^{-} = V_{dqs-}^{-} + V_{dqs+}^{+}.e^{2j\omega_e t} \tag{4}$$

where the subscripts (+) and (-) indicate positive and negative sequence components. The rotor voltages can be described similarly.

IV. Rotor Side Control

Using the equations for positive and negative sequence voltages and currents the apparent power of the converter can be calculated to improve the effects of voltage unbalance. The stator output apparent power can be described in the positive sequence reference frame as [4, 7]:

$$S = P_S + jQ_S = -\frac{3}{2} V_{dqs}^{+} I_{dqs}^{+*} \tag{5}$$

where the superscript (+) indicates the positive sequence reference frame and $V_{dq}^{+} = V_d^{+} + jV_q^{+}$ and $I_{dq}^{+} = I_d^{+} + jI_q^{+}$. Equation (5) can be expanded as [4, 5, 6, 9]:

$$S = -\frac{3}{2L_s}\begin{pmatrix} \left(V_{dqs+}^{+} + V_{dqs-}^{-}.e^{-j2\omega_e t}\right)\left(I_{dqs+}^{+*} + (I_{dqs-}^{-}.e^{-j2\omega_e t})^{*}\right) \\ -L_m.\left(V_{dqs+}^{+} + V_{dqs-}^{-}.e^{-j2\omega_e t}\right)\left(I_{dqr+}^{+*} + (I_{dqr-}^{-}.e^{-j2\omega_e t})^{*}\right) \end{pmatrix} \tag{6}$$

When (6) is multiplied out and expanded in term of d and q positive and negative terms, the terms for active and reactive power can be obtained as:

$$S = P_s + jQ_s = \left(P_{so\_av} + P_{s\sin 2}\sin(2\omega_s t) + P_{s\cos 2}\cos(2\omega_s t)\right) + j\left(Q_{so\_av} + Q_{s\sin 2}\sin(2\omega_s t) + Q_{s\cos 2}\cos(2\omega_s t)\right) \tag{7}$$

where P_{so}, $P_{s\ sin2}$, *and* $P_{s\ cos2}$, are the dc average, sine and cosine terms respectively, of twice the network frequency contained in the stator active power. The stator reactive components are similarly defined. The coefficients of (7) can be described as:

$$\begin{bmatrix} P_{so\_av} \\ Q_{so\_av} \\ P_{s\_\sin 2} \\ P_{s\_\cos 2} \\ Q_{s\_\sin 2} \\ Q_{s\_\cos 2} \end{bmatrix}_o = -\frac{3}{2\omega_e L_s}\begin{bmatrix} V_{ds+}^{+} & V_{qs+}^{+} & V_{ds-}^{-} & V_{qs-}^{-} \\ V_{qs+}^{+} & -V_{ds+}^{+} & V_{qs-}^{-} & -V_{ds-}^{-} \\ V_{qs-}^{-} & -V_{ds-}^{-} & -V_{qs+}^{+} & V_{ds+}^{+} \\ V_{ds-}^{-} & V_{qs-}^{-} & V_{ds+}^{+} & V_{qs+}^{+} \\ -V_{ds-}^{-} & -V_{qs-}^{-} & V_{ds+}^{+} & V_{qs+}^{+} \\ V_{qs-}^{-} & -V_{ds-}^{-} & V_{qs+}^{+} & -V_{ds+}^{+} \end{bmatrix}\left(\begin{bmatrix} V_{ds+}^{+} \\ V_{qs+}^{+} \\ V_{ds-}^{-} \\ V_{qs-}^{-} \end{bmatrix} + \omega_e L_m \begin{bmatrix} I_{dr+}^{+} \\ I_{qr+}^{+} \\ I_{dr-}^{-} \\ I_{qr-}^{-} \end{bmatrix}\right) \tag{8}$$

Because the d^+ axis is aligned with the positive sequence stator voltage vector (Fig. 2) the q axis component $V_{qs+}{}^{+} = 0$. In this paper only the real power oscillating components are being investigated and so by allowing $P_{s\_sin2} = 0$ and $P_{s\_cos2} = 0$ in (8) the negative sequence rotor currents can be controlled as:

$$I_{qr-}^{-} = \frac{2.v_{qs-}^{-}}{\omega_e L_m} + \frac{1}{V_{ds+}^{+}}\left(V_{ds-}^{-} I_{qr+}^{+} - V_{qs-}^{-} I_{dr+}^{+}\right) \tag{9}$$

$$I_{dr-}^{-} = -\frac{2.V_{ds-}^{-}}{\omega_e L_m} + \frac{1}{V_{ds+}^{+}}\left(V_{qs-}^{-} I_{qr+}^{+} - V_{ds-}^{-} I_{dr+}^{+}\right) \tag{10}$$

Compensating terms can also be obtained to control torque pulsations. By analysing the equation for torque, a similar analysis can be progressed and compensating currents I_{dr-}^{-} and I_{qr-}^{-} can be obtained to control the sine and cosine torque pulsations T_{s_sin2} and T_{s_cos2}. The electromagnetic torque in a DFIG can be described as [9]:

$$T_e = \frac{3}{2}\frac{p}{L_s \omega_e}\left(V_{dqs}(t).I_{dqr}^{*}(t)\right) \tag{11}$$

$$= T_{eo\_av} + T_{e\_\sin 2}\sin(2\omega_e t) + T_{e\_\cos 2}\cos(2\omega_e t) \tag{12}$$

Where the components T_{eo_av} , T_{e_sin2} and T_{e_cos2} can be expanded as [9]:

$$\begin{bmatrix} T_{so\_av} \\ T_{s\_\sin 2} \\ T_{s\_\cos 2} \end{bmatrix} = -\frac{3p}{2\omega_e L_s}\begin{bmatrix} V_{qs+}^{+} & -V_{ds+}^{+} & V_{qs-}^{-} & -V_{ds-}^{-} \\ -V_{ds-}^{-} & -V_{qs-}^{-} & V_{ds+}^{+} & V_{qs+}^{+} \\ V_{qs-}^{-} & -V_{ds-}^{-} & V_{qs+}^{+} & -V_{ds+}^{+} \end{bmatrix}\begin{bmatrix} I_{dr+}^{+} \\ I_{qr+}^{+} \\ I_{dr-}^{-} \\ I_{qr-}^{-} \end{bmatrix} \tag{13}$$

To reduce the torque pulsations the required control currents can be obtained by allowing $T_{s\_sin2} = 0$ and $T_{s\_cos2} = 0$ in (13). The negative sequence rotor control currents can then be obtained as:

$$I_{dr-}^{-} = \frac{1}{V_{ds+}^{+}}\left(V_{ds-}^{-} I_{dr+}^{+} + V_{qs-}^{-} I_{qr+}^{+}\right) \tag{14}$$

$$I_{qr-}^{-} = \frac{1}{V_{ds+}^{+}}\left(V_{qs-}^{-} I_{dr+}^{+} - V_{ds-}^{-} I_{qr+}^{+}\right) \tag{15}$$

The rotor currents are transformed into the positive sequence dq^+ and negative dq^- sequence reference frames, using the slip angle θ_{sl}. Band-stop (notch) filters tuned at $2\omega_e$ are then used to remove the oscillating terms, and leave the respective positive and negative sequence $I_{dqr}{}^{+}{}_{+}$ and $I_{dqr}{}^{-}{}_{-}$ control currents.

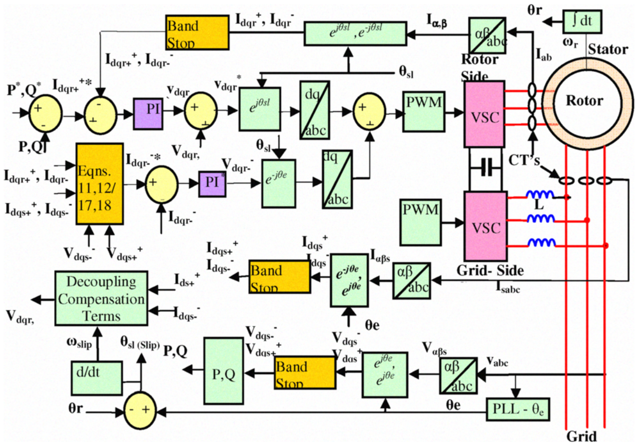

Fig. 3. Rotor Side Converter Parallel Unbalance Control Structure

It is also necessary to incorporate positive and negative sequence components, $I_{dqs}{}^{+}{}_{+}$ and $I_{dqs}{}^{-}{}_{-}$ respectively to obtain the necessary decoupling terms, $V_{d\ comp}$ and $V_{q\ comp}$. The control scheme is shown in Fig. 3 and further details of the rotor side control scheme can be obtained in [9].

V. GRID SIDE CONVERTER CONTROL

The control structure for the grid-side converter is based on the decoupled *d-q* vector control methods as previously outlined for the rotor-side converter. The grid-side converter controls the dc link voltage and can also control reactive power. Fig. 4 shows the grid side converter connected between the dc link and the grid.

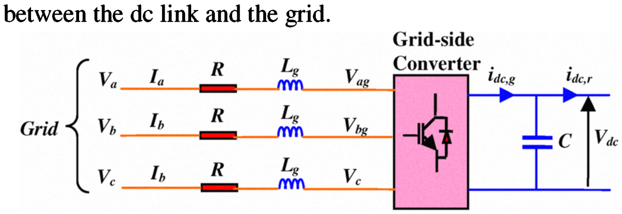

Fig. 4. Grid Side Converter

The *d-q* voltage equations can be obtained in the grid voltage reference frame with the d_{axis} aligned with the grid voltage as:

$$v_{dg}^{e} = i_{dg}^{e} R_g + L_g \frac{di_{dg}^{e}}{dt} - \omega_e L_g\ i_{qg}^{e} + v_{dg}^{e} \qquad (16)$$

$$v_{qg}^{e} = i_{qg}^{e} R_g + L_g \frac{di_{qg}^{e}}{dt} - \omega_e L_g\ i_{dg}^{e} + v_{qg}^{e} \qquad (17)$$

In addition under voltage unbalance conditions, there is in addition to dq^{+} coordinates there is also dq^{-} coordinates. Equations (18) and (19) below include the positive and negative sequence components.

$$v_{dqg+}^{+} = i_{dqg+}^{+} R_g + L_g \frac{di_{dqg+}^{+}}{dt} - \omega_e L_g\ i_{dqg+}^{+} + v_{dqg1+}^{+} \qquad (18)$$

$$v_{dqg-}^{-} = i_{dqg-}^{-} R_g + L_g \frac{di_{dqg-}^{-}}{dt} - \omega_e L_g\ i_{dqg-}^{-} + v_{dqg1-}^{-} \qquad (19)$$

Where (+) and (-) indicate positive and negative sequence components respectively. Using the equations for positive and negative sequence voltages and currents the apparent power of the converter can be power can be described as [8]:

$$S = P_g + jQ_g = \frac{3}{2} V_{dqg}^{+} I_{dqg}^{+*} \qquad (20)$$

And using (3) and (4):

$$S = \frac{3}{2} \cdot \left(\begin{array}{l} \left(V_{dqg+}^{+} + V_{dqg-}^{-} . e^{-j2\omega_e t}\right) . \\ \left(I_{dqg+}^{+*} + (I_{dqg-}^{-} . e^{-j2\omega_e t})^{*}\right) \end{array} \right) \qquad (21)$$

Multiplying eqn. (21) and expanding:

$$\begin{aligned} S = \Big\{ & \left(V_{dg+}^{+} . I_{dg+}^{+} - V_{dg+}^{+} . jI_{dg+}^{+} + jV_{qg+}^{+} . I_{dg+}^{+} + V_{qg+}^{+} . I_{qg+}^{+}\right) \\ & + \left(V_{dg+}^{+} . I_{dg-}^{-} - V_{dg+}^{+} . jI_{dg-}^{-} + jV_{qg+}^{+} . I_{dg-}^{-} + V_{qg+}^{+} . I_{qg-}^{-}\right) e^{j2\omega_e t} \\ & + \left(V_{dg-}^{-} . I_{dg+}^{+} - jV_{dg-}^{-} . I_{qg+}^{+} + jV_{qg-}^{-} . I_{dg+}^{+} + V_{qg-}^{-} . I_{qg+}^{+}\right) e^{-j2\omega_e t} \\ & + \left(V_{dg-}^{-} . I_{dg-}^{-} - V_{dg-}^{-} . jI_{dg-}^{-} + jV_{qg-}^{-} . I_{dg-}^{-} + V_{qg-}^{-} . I_{qg-}^{-}\right) \Big\} \end{aligned} \qquad (22)$$

Equation (22) can be equated to:

$$P_{acg} = P_{og} + P_{c2g}\cos(2\omega_s t) + P_{s2g}\sin(2\omega_s t)$$

$$Q_{acg} = Q_{og} + Q_{c2g}\cos(2\omega_s t) + Q_{s2g}\sin(2\omega_s t) \qquad (23)$$

Where:

$$\begin{bmatrix} P_{og} \\ Q_{og} \\ P_{c2g} \\ P_{s2g} \\ Q_{c2g} \\ Q_{s2g} \end{bmatrix} = \frac{3}{2} \begin{bmatrix} V_{dg+}^{+} & V_{qg+}^{+} & V_{dg-}^{-} & V_{qg-}^{-} \\ V_{qg+}^{+} & -V_{dg+}^{+} & V_{qg-}^{-} & -V_{dg-}^{-} \\ V_{dg-}^{-} & V_{qg-}^{-} & V_{dg+}^{+} & V_{qg+}^{+} \\ V_{qg-}^{-} & -V_{dg-}^{-} & -V_{qg+}^{+} & V_{dg+}^{+} \\ V_{qg-}^{-} & -V_{dg-}^{-} & V_{qg+}^{+} & -V_{dg+}^{+} \\ -V_{dg-}^{-} & -V_{qg-}^{-} & V_{dg+}^{+} & V_{qg+}^{+} \end{bmatrix} \begin{bmatrix} I_{dg+}^{+} \\ I_{qg+}^{+} \\ I_{dg-}^{-} \\ I_{qg-}^{-} \end{bmatrix} \qquad (24)$$

VI. COORDINATED CONTROL

Earlier it was observed that the stator power oscillations can be improved by controlling the negative sequence control currents as in equations (9) and (10) to control $P_{s\_sin2} = P_{s\_cos2} = 0$. The torque pulsations were controlled using equations (14) and (15) to control the double frequency torque pulsations T_{e_sin2} and T_{e_cos2}. However it can be observed in these four equations that it is not possible to control both the power and torque pulsations simultaneously.

A method to control both the power oscillations and the torque pulsations in a DFIG, by analysing the rotor side converter which controls the stator power in the stator flux oriented reference frame and the control of the grid side converter in the grid voltage reference frame was investigated in [10]. However in contrast to stator flux oriented control SFO, stator voltage oriented control SVO can result in the system stability and damping being independent of the rotor current. The total apparent power of a DFIG is [6]:

$$S = P_T + jQ_T = -\frac{3}{2}\left(V_{dqs}^{+} I_{dqs}^{*} + V_{dqr}^{+} I_{dqr}^{*}\right) \qquad (25)$$

The total real power in equation (25) is $P_T = P_s + P_g$. From (7) and knowing that $S_g = P_g + jQ_g$ and observing (23) the total real power can be described as:

$$P_T = \left(P_{s\_av} + P_{s\_\sin 2}\sin(2\theta_e) + P_{s\_\cos 2}\cos(2\theta_e)\right) + \left(P_{og} + P_{s2g}\sin(2\theta_g) + P_{c2g}\cos(2\theta_g)\right) \tag{26}$$

The rotor side converter and the grid side converter are both controlled in the grid or stator voltage reference frame, see Fig. 2 and therefore $\theta_e = \theta_g$ and eqn. (26) can be described as:

$$P_T = (P_{s\_av} + P_{og}) + (P_{s\_\sin 2} + P_{s2g})\sin(2\theta_e) + (P_{s\_\cos 2} + P_{c2g})\cos(2\theta_e t) \tag{27}$$

If in (27) letting P_{s_sin2} = $-P_{s2g}$ and P_{c_cos2} = $-P_{c2g}$ then the total real power becomes P_T = $(P_{s\_av}+P_{og}$). For P_{s2g} = $-P_{s\_sin2}$, observing (24) and (8) and with the rotor side converter d-axis aligned with stator or grid voltage and the grid side converter d-axis also aligned with the grid voltage will result in $V_{qs}{}^{+}{}_{+} = V_{qg}{}^{+}{}_{+} = 0$ and (27) becomes:

$$P_{s2g} = \frac{3}{2}\left(V^-_{qg-}I^+_{dg+} - V^-_{dg-}I^+_{qg+} - 0 + V^+_{dg+}I^-_{qg-}\right) = \left\{ -P_{s\_\sin 2} = \frac{3}{2\omega_e L_s}\left(V^-_{qs-}V^+_{ds+} + 0 + 0 + V^+_{ds+}V^-_{qs-}\right) - \frac{3L_m}{2L_s}\left(V^-_{qs-}I^+_{dr+} - V^-_{ds-}I^+_{qr+} + 0 + V^+_{ds+}I^-_{qr-}\right)\right\} \tag{28}$$

And solving (28) to get the grid side $I_{qg}{}^{-}{}_{-}$:

$$I^-_{qg-} = \frac{1}{V^+_{dg+}}\left[-V^-_{qg-}I^+_{dg+} + V^-_{dg-}I^+_{qg+}\right] + \frac{2}{\omega_e L_s V^+_{dg+}}\left(V^-_{qs-}V^+_{ds+}\right) - \frac{L_m}{L_s V^+_{dg+}}\left(V^-_{qs-}I^+_{dr+} - V^-_{ds-}I^+_{qr+} + V^+_{ds+}I^-_{qr-}\right) \tag{29}$$

Similarly For $P_{s\_cos2} = -P_{c2g}$, from (8) and (24):

$$P_{s\_\cos 2} = -\frac{3}{2\omega_e L_s}\left(V^-_{ds-}V^+_{ds+} + 0 + V^+_{ds+}V^-_{ds-} + 0\right) + \frac{3L_m}{2L_s}\left(V^-_{ds-}I^+_{dr+} + V^-_{qs-}I^+_{qr+} + V^+_{ds+}I^-_{dr-} + 0\right) =$$

$$-P_{c2g} = -\frac{3}{2}\left[V^-_{dg-}.I^+_{dg+} + V^-_{qg-}.I^+_{qg+} + V^+_{dg+}.I^-_{dg-} + 0\right] = 0 \tag{30}$$

And solving (30) to get the grid side negative sequence I_q control reference yields:

$$I^-_{dg-} = -\frac{1}{V^+_{dg+}}\left[V^-_{qg-}.I^+_{dg+} + V^-_{dg-}.I^+_{qg+}\right] + \frac{2}{V^+_{dg+}\omega_e L_s}\left(V^+_{ds+}V^-_{ds-}\right) - \frac{L_m}{V^+_{dg+}L_s}\left(V^-_{ds-}I^+_{dr+} + V^-_{qs-}I^+_{qr+} + V^+_{ds+}I^-_{dr-}\right) \tag{31}$$

VII. SIMULATION RESULTS

The control scheme of the grid side converter in Fig.5 was implemented in a model in the software program Matlab/Simulink. A timed switch introduced a single-phase load at 0.4 seconds (Fig. 1). Fig. 6 shows plots of the stator power and torque when compensation control is applied to the rotor side converter to control power oscillations only.

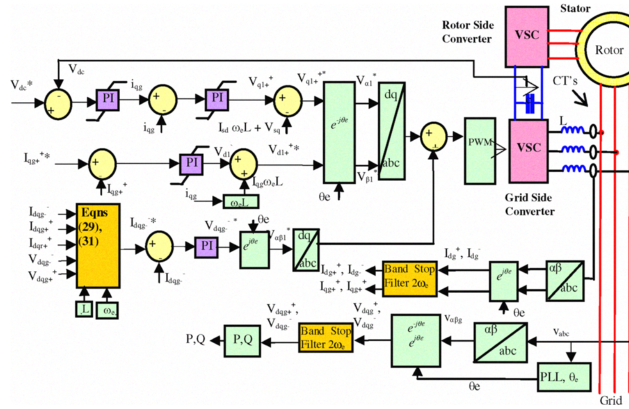

Fig. 5. Grid Side Converter Control

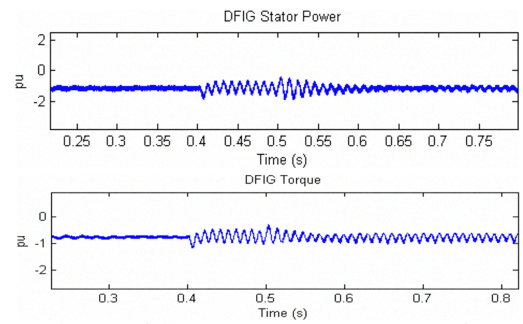

Fig. 6. DFIG Stator Power and Torque – Power Comp.

The steady state power is set at (-1.0) pu and as observed in Fig 6 when voltage unbalance is applied at 0.4s the power oscillates at twice the network frequency (100 Hz). The compensation control scheme was timed to start at 0.5 seconds, with the negative sequence currents controlled according to the requirement to minimise power pulsations. It can be observed that after about 0.65 seconds the power oscillations are practically eliminated, however there is still a reasonable magnitude of torque pulsations.

Fig. 7 is a plot of stator power and torque when compensation control is applied to the rotor side converter to control torque oscillations only. When voltage unbalance is introduced at 0.4s power and torque oscillations occur at twice the network frequency, and at 0.5s when torque compensation is introduced the torque pulsations decay substantially, however the power still has appreciable oscillations.

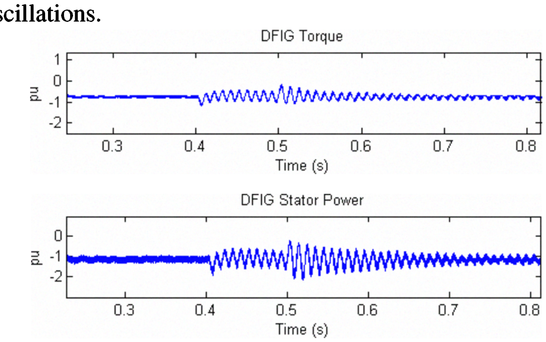

Fig. 7. DFIG Stator Power and Torque – Torque Comp.

The total power supplied by the DFIG is plotted in Fig. 8. The DFIG is this case is controlled to reduce the torque pulsations. When torque compensation is applied at 0.5s there is only a slight decrease in the total power oscillations.

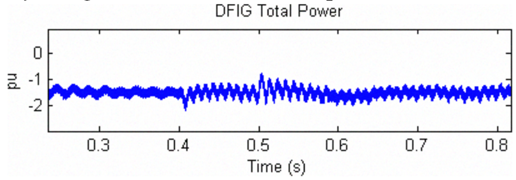

Fig. 8. DFIG Total Power – No Grid Side compensation

Fig. 9 is a plot of the total power supplied by the DFIG with the rotor side converter controlling torque and grid side converter now controlled to reduce the total power oscillations. It is clear that there is a good improvement in the reduction of power oscillations at around 0.65s.

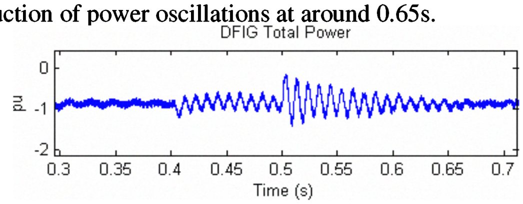

Fig. 9. DFIG Total Power – Grid Side compensation

The total current supplied by the DFIG is shown in Fig. 10. It is clear that when voltage unbalance is introduced at 0.4s the current unbalance is significant, and when the compensation schemes are switched in at 0.5s the current unbalance decreases and is much reduced at around 0.8s.

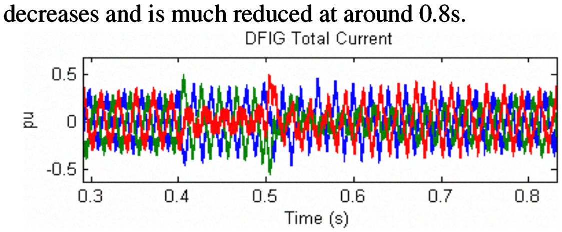

Fig. 10. DFIG Total Current

Similarly the stator current unbalance is also improved as observed in Fig. 11.

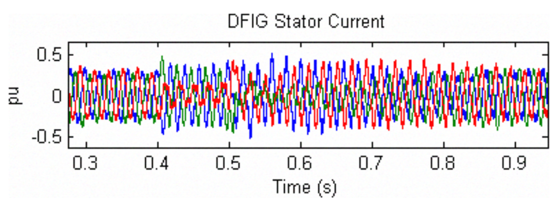

Fig. 11. Stator Current

VIII. CONCLUSION

A Control structure to improve and mitigate the detrimental effects of voltage unbalance on a DFIG rotor-side and grid-side converter was investigated. In particular modifications to the control structure of the grid side converter was implemented to reduce the total power oscillations on the stator and the grid side converter.

A model of a DFIG was implemented in Matlab/Simulink to incorporate compensating control structures for the rotor-side and grid side converter to reduce power and torque pulsations. The simulation results demonstrate the improvement in the behaviour of the DFIG to network voltage unbalance when a coordinated compensation structure was introduced. If this type of control were implemented it is clear that an improvement would result in the behaviour of DFIG's during network voltage unbalance conditions.

IX. APPENDIX A

V_{dqs}^{+}, V_{dqs}^{-} = Stator dq voltages in the positive and negative sequence reference frames.

I_{dqs}^{+}, I_{dqs}^{-} = Stator dq currents in the positive and negative sequence reference frames.

I_{dqr}^{+}, I_{dqr}^{-} = Rotor dq currents in the positive and negative sequence reference frames.

ψ_{dqs}^{+}, ψ_{dqs}^{-} = Stator dq flux linkages in the positive and negative sequence reference frames

ψ_{dqr}^{+}, ψ_{dqr}^{-} = Rotor dq flux linkages in the positive and negative sequence reference frames

R_s, L_s = Stator winding resistance and leakage inductance

L_m = Magnetising inductance.

$R_r^{`}$, $L_r^{`}$ = Rotor referred winding resistance and inductance

R_g, L_g = Grid side filter resistance and inductance

REFERENCES

1. A Larson, *The Power Quality of Wind Turbines*, PhD. Dept. of Electrical Power Engineering, Chalmers University of Technology, Gothenburg, Sweden 2000.
2. Matlab. The Mathworks Inc.
3. M.F. Conlon and J. Kearney, "Negative Sequence Analysis of Induction Machines" 40th Universities Power Engineering Conference (UPEC), Cork, Ireland, 6th - 9th September 2005
4. Lie Xu, Yi Wang, "Dynamic Modelling and Control of DFIG-Based Turbines Under Unbalanced Network Conditions", *IEEE Transactions on Power Systems*, 2007. pp 314-323.
5. Yi Wang, Lie Xu, "Control of DFIG-Based Wind Generation Systems under Unbalanced Network Supply", *IEEE International, Electrical Machines and Drives Conference*, 2007, IEMDC 3-5th May '07. pp 430-435.
6. Jeong-Ik Jang, Young-Sin Kim, "Active and Reactive Power Control of DFIG for Wind Energy Conversion under Unbalanced Grid Voltage", *IEEE IPEMC Conference* 2006.
7. Hu Jia-bing, He Yi-kang, "Enhanced control of DFIG-using back-to-back PWM VSC under unbalanced grid voltage conditions", *Journal of Zhejiang University SCIENCE A,* China, 2007. pp 1330-1339.
8. Hong-Seok Song, Kwanghee Nam, "Dual Current Control for PWM Converter Under Unbalanced Input Voltage Conditions", *IEEE Transactions on Industrial Electronics*, vol. 46 no. 5, October 1999, pp 953-959.
9. J Kearney, M. F. Conlon, "Control Double-Fed Induction Generator Wind Turbine During Network Voltage Unbalance Conditions", *42nd Universities Power Engineering Conference (UPEC)*, Padua, Italy, 2nd - 5th September 2008.
10. Lie XU, "Coordinated Control of DFIG's Rotor and Grid Side Converters During Network Unbalance", *IEEE Transactions on Power Electronics,* vol. 23, no. 3, May 2008.